Thermoelectricity at Molecular Length scale: A New Perspective

Moumita Dey[a*], Ishani Mukherjee[a]

ABSTRACT

The project deals with a thorough analysis of thermoelectric phenomenon in a magnetic helix possessing long range hopping (LRH) interactions. The magnetic helix is subjected to a circularly polarized light irradiation which plays the central role in our analysis. Simulating the quantum system within a Tight-binding framework, we evaluate all the thermoelectric quantities using Landauer prescription, and the two-terminal transmission probabilities are determined following the robust Green's function technique. The effect of irradiation is incorporated following Bloch-Floquet prescription using minimal coupling scheme through the hopping term. Quite interestingly we find that, electrical conductance as well as thermopower increases significantly at some typical Fermi energies whereas the thermal conductance due to electrons gets reduced at these energies, resulting a large figure of merit. The underlying physical mechanism of achieving large figure of merit (ZT ~ 4) relies on the asymmetric transmission function in such a LRH magnetic helix which is further enhanced in presence of light irradiation. In presence of the spin-dependent scattering, the up and down spin energy channels gets separated which leads to several interesting features in thermoelectric phenomena. Our analysis might be helpful in studying thermoelectric behaviour in different kinds of helical geometries and similar kind of fascinating systems having long range hopping interactions.

I. Introduction

To address the energy crisis across the globe conversion of waste heat into usable electrical energy has been considered as one of the major challenges both in science and technology over the past few [1].

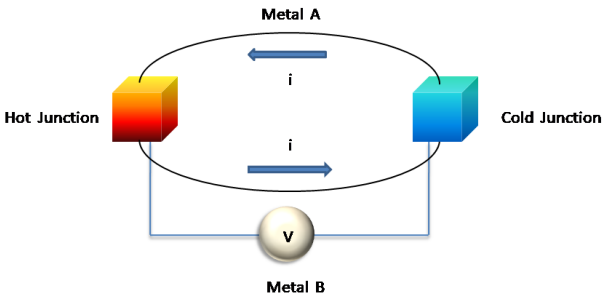

Figure 1: Schematic diagram of Seebeck effect where a thermal gradient induces a voltage drop at two junctions.

Out of many possible techniques, *Thermoelectric* (TE) energy conversion has been considered as one of the

*Department of Physics,
School of Basic and Applied Sciences,
Adamas University, Kolkata – 700126, India,
Email: moumita.dey@adamasuniversity.ac.in

most sought after method because of the 'green' nature of conversion process.

First thermoelectric effect, popularly known as Seebeck effect [2], discovered way back in 1822, where a voltage drop is induced across the dissimilar metallic junctions kept at two different temperatures (see Fig. 1.1). Thus, heat energy is being converted into electrical energy through this process. If ΔV is the amount of voltage generated due to temperature difference ΔT, then the Seebeck co-efficient is defined as

$$S = -\frac{\Delta V}{\Delta T} \quad (1)$$

Twelve years later, Peltier [4] noticed just the opposite phenomenon, i.e., temperature gradient is being induced when a current is passing through a metallic junction. If Q amount of heat is generated or absorbed due to current I flowing through a metallic branch, then these two factors are related as $Q = \Pi I$ where Π being the Peltier co-efficient.

Few years later Lenz suggested by simple experimental demonstration that the thermoelectric effect can be utilized for both power generation and refrigeration [3].

Now, if a thermoelectric material is coupled to two heat baths having the temperatures T_h (temperature of the hot junction) and T_c (temperature of the cold junction) ($T_h > T_c$), then from the argument of thermodynamics it is shown that the efficiency of thermoelectric power generation can be written as

$$\eta_{\max} = \left(1 - \frac{T_c}{T_h}\right)\left(\frac{r-1}{r+\frac{T_c}{T_h}}\right) \quad (2)$$

where, $r = \sqrt{1+ZT}$.

Here, T is the equilibrium temperature and defined as, $T = \frac{T_c + T_h}{2}$.

The parameter ZT, a dimensionless quantity, is called the ***Figure of Merit*** (FOM), which plays the crucial role in determining the quality of the thermoelectric material used. If the value of ZT is increased, $\eta_{\max}$ approaches the ideal Carnot cycle efficiency.

The FOM is defined as,

$$ZT = \frac{GS^2T}{\kappa} \quad (3)$$

Here, G represents the electrical conductance of the material, S describes the Seebeck co-efficient and κ corresponds to thermal conductance of the functional material and it includes both electronic and phononic contributions i.e., $\kappa = \kappa_{el} + \kappa_{ph}$.

Now, as metals were unable to produce FOM even of the order of unity, so the attention got shifted to bulk semiconductors. So far lots of thermoelectric materials have been taken into account like Bi_2Te_3, Mn-Si,Bi-Sb-Te-Se and to name a few. But, in most of the cases ZT is quite close to unity at room temperature, and for bulk samples it has not been possible to enhance ZT very much, which was also the theoretical prediction. To enhance ZT lower thermal conductance (κ) and at the same time higher electrical conductance (G) and Seebeck coefficient (S) is preferred. To obtain low thermal conductance, quantum confinement was an appropriate option. So, attention is shifted to quantum wires and molecular junctions, which are even smaller in size than regular quantum systems, as the prospective thermoelectric materials [7, 8].

The availability, low-dimensionality, and low thermal conductivity make the molecular systems a natural choice for next generation thermoelectric materials with enhanced ZT. As molecules are automatically nanostructured and their electrical conductance (G) and Seebeck co-efficient (S) can be monitored externally by applying a suitable gate voltage and/or some other possible ways, they can be chosen as potential candidates for efficient and high power thermoelectric devices [9-20].

Till date quite a number of calculations were carried out where thermoelectric properties of molecular junctions were studied extensively mostly within the framework of ballistic transport theory. In 2015, Dubi *et al.* have proposed [24] a new way to tune and enhance ZT of a molecular junction by introducing semiconducting nanoparticles within the junction, thereby making a hybrid single molecule-nanoparticles junction. In another work, Galperin *et al.* have proposed [26] a simple phenomenological model to

investigate inelastic scattering effects at molecular scale level that can influence the thermopower.

From the recent experimental findings of thermopower measurements in nano-wires [21, 27, 28, 29], it has been established that there is a possibility of enhancement of *S* and *G* and reduction of κ independently by designing a system which is smaller than phonon mean free path and larger than electronic mean free path (or holes in case), and thus, there exists a finite possibility to get enhanced and favourable ZT .

Very few experiments have been performed so far on molecular junctions for measuring thermo power. Among them in 2007, Reddy *et al.* have done an experiment [30] which demonstrates that the Seebeck co-efficient (*S*) and the electrical conductance (G) can be increased simultaneously by applying a gate voltage i.e., by shifting equilibrium Fermi level closer to the resonant peak. It strongly suggests that much higher ZT can be achieved in molecular systems.

The next challenge is to find which molecule and/or the material junction leads to the best and experimentally achievable thermoelectric properties. Keeping this in mind, we choose a magnetic helix mimicking a helical molecule (like ss DNA, α protein etc.) that exhibits several interesting features and especially in presence of external irradiation.

II. Theoretical Formulation and Numerical Simulation

Following the Landauer-Buttiker formalism, the Seebeck coefficient, electrical and thermal conductance can be written in terms of transmission probability as Seebeck coefficient is given by

$$S = -\frac{1}{eT}\frac{\int \tilde{T}_{12}(E)(E-\mu)\frac{\partial f}{\partial E}dE}{\int \tilde{T}_{12}(E)\frac{\partial f}{\partial E}dE} \quad (4)$$

$$G = -\frac{2e^2}{h}\int \tilde{T}_{12}(E)\frac{\partial f}{\partial E}dE \quad (5)$$

$$\kappa_{el} = \frac{2}{hT}\left[L_2 - \frac{L_1^2}{L_0}\right] \quad (6)$$

where, $L_n = \int_{-\infty}^{\infty}(E-\mu)^n \tilde{T}(E)\frac{\partial f}{\partial E}dE$ are the Landauer Integrals.

The Tight binding Hamiltonian of the ss Magnetic Helix (MH) in Wannier basis can be written as

$$H_{helix} = \sum_{n=1}^{N} c_n^{\dagger}\left(\varepsilon_n - \vec{h}.\vec{\sigma}\right)c_n + \sum_{n=1}^{N-1}\sum_{j=1}^{N-n}\left[c_n^{\dagger}\tilde{t}_{nj}c_{n+j} + c_{n+j}^{\dagger}\tilde{t}_{nj}^{\dagger}c_n\right]$$

(7)

where, $c_n^{\dagger}$ and c_n the creation and annihilation operations respectively at n-th site. In Wannier basis considering spin degree of freedom it takes the form as,

$$c_n^{\dagger} = \begin{pmatrix} c_{n\uparrow}^{\dagger} & c_{n\downarrow}^{\dagger} \end{pmatrix} \text{ and } c_n = \begin{pmatrix} c_{n\uparrow} \\ c_{n\downarrow} \end{pmatrix}$$

Hence, ε_n and $\tilde{t}_{nj}$ describes the on-site energy and hopping between n-th and (n+j)-th site respectively in presence of high frequency ($\hbar\omega >> t_{nj}$) transverse irradiation. In spin Wannier basis it looks as,

$$\varepsilon_n = \begin{pmatrix} \varepsilon_n & 0 \\ 0 & \varepsilon_n \end{pmatrix} \text{ and } \tilde{t}_{nj} = \begin{pmatrix} t_{nj}J_0(\Gamma) & 0 \\ 0 & t_{nj}J_0(\Gamma) \end{pmatrix}$$

$\vec{h}.\vec{\sigma}$ represents the interaction of the spin ($\vec{\sigma}$) of the itinerant electrons with the localized magnetic moments ($\vec{h}$) associated with n-th site. Using spherical polar coordinates the magnetic moment h can be expressed as,

$$\vec{h} = h\sin\theta\cos\phi\,\hat{i} + h\sin\theta\sin\phi\,\hat{j} + h\cos\theta\,\hat{k}$$

and the full form of this term is given as

$$\begin{aligned}\vec{h}.\vec{\sigma} &= h_x\sigma_x + h_y\sigma_y + h_z\sigma_z \\ &= h\sin\theta\cos\phi\begin{pmatrix}0 & 1\\ 1 & 0\end{pmatrix} + h\sin\theta\sin\phi\begin{pmatrix}0 & -i\\ i & 0\end{pmatrix} + h\cos\theta\begin{pmatrix}1 & 0\\ 0 & -1\end{pmatrix} \\ &= \begin{pmatrix} h\cos\theta & -h\sin\theta e^{-i\phi} \\ h\sin\theta e^{i\phi} & -h\cos\theta \end{pmatrix}\end{aligned}$$

Here, t_{nj} denotes the long range hopping between n-th and (n+j)-th sites. Following Slater-Koster scheme, the it can be written as,

$$t_{nj} = t_{11}e^{-(l_{nj}-l_{11})/l_c} \quad (8)$$

Here, l_{nj} is the distance between n-th and (n+j)-th sites and mathematically it is given by

$$l_{nj} = \sqrt{4R^2\sin^2\left(\frac{j\Delta\varphi}{2}\right) + (j\Delta h)^2} \quad (9)$$

Here, $\Delta\varphi$, Δh and R are the twisting angle, stacking height and radius of the helix respectively. Following

the above equation the distance between first two sites are $l_{11} = \sqrt{4R^2 \sin^2\left(\frac{\Delta\varphi}{2}\right) + (\Delta h)^2}$

Now if the system is being irradiated externally then the effect of the e. m. radiation is incorporated in the system with the help of Bloch-Floquet formalism. It can be shown by a detailed calculation that, the renormalized hopping between the *m-th* and *n-th* sites in presence of external irradiation, i.e., periodically driven electric field (magnitude of the magnetic field associated with e. m. radiation is too small compared to the electric field and it can be ignored.) can be written as,

$$\tilde{\tau}_{m,n}^{p,q} = \frac{1}{T}\int_0^T \tau_{mn}\, e^{i\left(\vec{k}+\vec{A}\right)\cdot\left(\vec{R}_m - \vec{R}_n\right)} e^{-i\omega t(p-q)}\, dt$$

So, finally, in presence of high frequency radiation (in transverse direction w.r.t. the helical axis), the modified hopping would be, $t_{nj} = t_{11}\, J_0(\Gamma) e^{-(l_{nj}-l_{11})/l_c}$.

To calculate the phase factor Γ, we need to calculate the distance between n-th and (n+j)-th sites of the helical molecule, i.e. to calculate the quantity $\left(\vec{R}_{n,j} - \vec{R}_n\right)$, we start with evaluating component wise. If we assume that the 1st site is placed on X axis, and each sites are placed at an angle $\Delta\varphi$ (known as the twisting angle) apart,

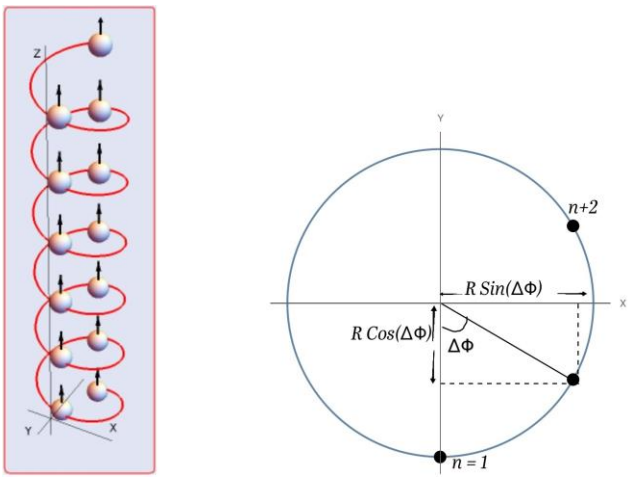

Fig 2: Schematic illustration of a single stranded helical molecules

then the X, Y and Z components of the n-th site can be written as follows,

$$X_n = R\cos\{(n-1)\Delta\varphi\}$$
$$Y_n = R\sin\{(n-1)\Delta\varphi\}$$
$$Z_n = (n-1)\Delta\varphi$$

Similarly, for the (n+j)-th site, the components are,

$$X_{n+j} = R\cos\{(n+j-1)\Delta\varphi\}$$
$$Y_{n+j} = R\sin\{(n+j-1)\Delta\varphi\}$$
$$Z_{n+j} = (n+j-1)\Delta\varphi$$

Therefore the X-component of the radius vector $\left(\vec{R}_{n,j} - \vec{R}_n\right)$ is given by,

$$\begin{aligned} a_x^{nj} &= X_{n+j} - X_n \\ &= R\left[\cos\{(n+j-1)\Delta\varphi\} - \cos\{(n-1)\Delta\varphi\}\right] \\ &= -2R\sin\left(\frac{n\Delta\varphi + j\Delta\varphi - \Delta\varphi + n\Delta\varphi - \Delta\varphi}{2}\right)\sin\left(\frac{n\Delta\varphi + j\Delta\varphi - \Delta\varphi - n\Delta\varphi + \Delta\varphi}{2}\right) \\ &= -2R\sin\left(n\Delta\varphi - \Delta\varphi + \frac{j\Delta\varphi}{2}\right)\sin\left(\frac{j\Delta\varphi}{2}\right) \end{aligned}$$

Similarly the Y and Z components are given by

$$\begin{aligned} a_y^{nj} &= Y_{n+j} - Y_n \\ &= R\left[\sin\{(n+j-1)\Delta\varphi\} - \sin\{(n-1)\Delta\varphi\}\right] \\ &= 2R\cos\left(\frac{n\Delta\varphi + j\Delta\varphi - \Delta\varphi + n\Delta\varphi - \Delta\varphi}{2}\right)\sin\left(\frac{n\Delta\varphi + j\Delta\varphi - \Delta\varphi - n\Delta\varphi + \Delta\varphi}{2}\right) \\ &= 2R\sin\left(n\Delta\varphi - \Delta\varphi + \frac{j\Delta\varphi}{2}\right)\sin\left(\frac{j\Delta\varphi}{2}\right) \end{aligned}$$

and,

$$\begin{aligned} a_z^{nj} &= Z_{n+j} - Z_n \\ &= j\,\Delta h \end{aligned}$$

So, $\vec{R}_{nj} - \vec{R}_n = a_x^{nj}\,\hat{i} + a_y^{nj}\,\hat{j} + a_z^{nj}\,\hat{k}$

If, the light is being incident along Y axis, then the Electric field ($\vec{E}$) and the corresponding magnetic vector potential ($\vec{A}$) lies in XZ plane. As we have considered the circularly polarized light, the analytical form of the vector potential can be written as, $\vec{A} = A_0\cos\omega t\,\hat{i} + A_0\sin\omega t\,\hat{k}$.

But because of the geometry of the system the incidence angle of the light changes along the circumference, and hence the effective magnetic vector potential can be written as,

$$\begin{aligned} \vec{A}_{eff} &= R_z(\Delta\varphi)\,\vec{A} \\ &= \begin{pmatrix} \cos\Delta\varphi & \sin\Delta\varphi & 0 \\ -\sin\Delta\varphi & \cos\Delta\varphi & 0 \\ 0 & 0 & 1 \end{pmatrix}\begin{pmatrix} A_x \\ 0 \\ A_z \end{pmatrix} \\ &= A_x\cos\Delta\varphi\,\hat{i} - A_x\sin\Delta\varphi\,\hat{j} + A_z\,\hat{k} \end{aligned} \qquad (10)$$

Therefore,

$$\begin{aligned}\vec{A}.\left(\vec{R}_{nj}-\vec{R}_n\right) &= A_x\cos\Delta\varphi\, a_x^{nj} - A_x\sin\Delta\varphi a_y^{nj} + A_z a_x^{nj} \\ &= A_0\cos\omega t\cos\Delta\varphi\, a_x^{nj} - A_0\cos\omega t\sin\Delta\varphi a_y^{nj} + A_0\cos\omega t\, a_x^{nj} \\ &= \sin\omega t\left(A_0\, a_z^{nj}\right) + \cos\omega t\left[A_0\cos\Delta\varphi\, a_x^{nj} - A_0\sin\Delta\varphi\, a_y^{nj}\right] \\ &= \Gamma\sin\left(\omega t+\psi\right)\end{aligned}$$

where,

$$\Gamma = A_0\sqrt{a_z{}^2 + a_x{}^2\cos^2\Delta\varphi + a_y{}^2\sin^2\Delta\varphi + a_x a_y\sin\left(2\Delta\varphi\right)} \quad (11)$$

and, $$\psi = \tan^{-1}\left(\frac{a_x\cos\Delta\varphi - a_y\sin\Delta\varphi}{a_z}\right) \quad (12)$$

Hence, in high frequency limit, the effective hopping from n-th site to (n+j)-th site becomes,

$$\tilde{t}_{nj} = t_{11}J_0\left(A_0\sqrt{a_z{}^2 + a_x{}^2\cos^2\Delta\varphi + a_y{}^2\sin^2\Delta\varphi + a_x a_y\sin\left(2\Delta\varphi\right)}\right)e^{-\left(l_{nj}-l_{11}\right)/l_c}$$

To evaluate transmission probability we adopt the Green's function technique using Landauer Büttiker formalism which applies well in linear response regime (low bias).

The non-magnetic semi-infinite leads attached to the two ends of the magnetic helix are described within the tight-binding approximation as,

$$H_{lead} = \sum_i c_i^{\dagger}\varepsilon_i c_i + \sum_i\left[c_i^{\dagger}t_l c_{i+1} + h.c.\right] \quad (13)$$

ε_l and t_l are the site energy and the nearest-neighbour hoping strength of the sites associated with the side attached leads respectively.

Finally the molecule-electrode coupling is represented by,

$$H_{coupling} = \left[c_0^{\dagger}\tau_1 c_1 + h.c.\right] + \left[c_{N+1}^{\dagger}\tau_2 c_N + h.c.\right] \quad (14)$$

The first term describes the source-to-molecule coupling whereas the second term describes the molecule-to-drain coupling.

Thus, the total Hamiltonian of the system is describes as,

$$H = H_{helix} + H_{leads} + H_{coupling} \quad (15)$$

Here, we will use the Green's function technique to evaluate the transmission probability.

In order to calculate the transmission probability we use single particle Green's function technique. Within the regime of coherent transport and for non-interacting system the technique is well applied.

The single particle Green's function operator representing the entire system for an electron with injecting energy E is defined [5] as,

$$\tilde{G}^r = \left(E - H + i\eta\right)^{-1} \quad (16)$$

where, $\eta \to 0^+$. Following the matrix form of H and $\tilde{G}$, the problem of finding $\tilde{G}$ in the full Hilbert space of H can be mapped exactly to a Green's function $\left(G^r\right)$ in the reduced Hilbert space of the molecule itself i.e.,

$$G^r = \left(E.1_{2N\times 2N} - H_{mol} - \sum_1 - \sum_2\right)^{-1} \quad (17)$$

where, $\sum_i = H_{i,coupling}^{\dagger}G_{lead}\,H_{i,coupling}$.

These, $\sum_1^{\sigma(\sigma')}$ and $\sum_2^{\sigma(\sigma')}$ are the spin dependent self-energy matrices introduced to incorporate the effect of coupling of the molecule to source and drain, respectively.

It can be shown that the analytic form of the non-zero term of the self-energy matrices are

$$\sum_{1(2)}^{\sigma(\sigma')} = \frac{\tau_{1(2)}{}^2}{2t_l{}^2}\left[\left(E-\varepsilon_l\right) - i\sqrt{4t_l{}^2 - \left(E-\varepsilon_l\right)^2}\right] \quad (16)$$

Following Fisher-Lee relation, the spin resolved transmission probability of an electron with spin σ and energy E from source to drain with spin σ' can be calculated as,

$$\tilde{T}^{\sigma\sigma'}\left(E\right) = Tr\left[\Gamma_1^{\sigma}G^r\Gamma_2^{\sigma'}G^a\right] \quad (17)$$

Here, $\Gamma_i^{\sigma(\sigma')}$'s (i = 1, 2) are spin dependent coupling matrices representing the coupling between the molecule and electrodes. $\Sigma_k^{\sigma(\sigma')}$ and $\Sigma_k^{\sigma(\sigma')\dagger}$ are the retarded and advanced spin dependent self-energies associated with k-th electrode, respectively.

The spin dependent coupling matrices can be obtained from the self-energy expression and is expressed as,

$$\Gamma_k^{\sigma} = -2\,\mathrm{Im}\left[\Sigma_k^{\sigma}\right]$$

III Numerical Simulation and Discussion

In this subsection we present our numerical results based on the above theoretical framework which

includes the study of electrical conductance (G), thermopower or Seebeck coefficient (S), thermal conductance due to electrons (κ_{el}) along with the Figure of Merit (ZT) in a single-strand Magnetic Helix (MH), subject to a circularly polarized irradiation. Both in the absence and presence of circularly polarized light, the thermoelectric quantities are evaluated.

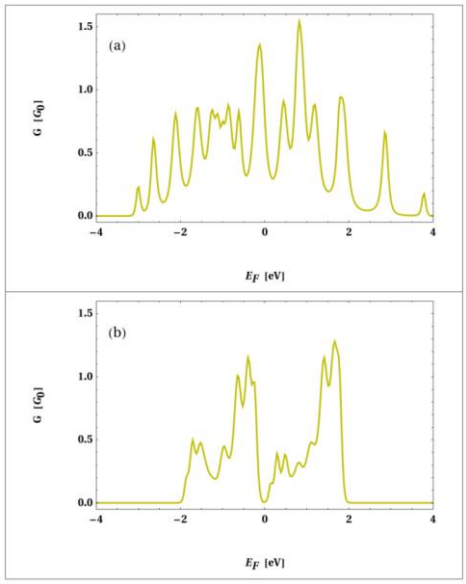

Figure 3: Electrical Conductance (measured in unit of G_0) as a function of Fermi Energy (E_F) for a long-range hopping (LRH) magnetic helix in (a) absence and (b) presence of light. Here, we set N = 10 and A_0 = 0.5.

The common set of parameter values, unless otherwise stated, are as follows. The radius of the Helix = $R = 7.0\,\text{Å}$, the decay exponent = $l_c = 0.9\,\text{Å}$, stacking distance between two nearest neighbor sites $\Delta h = 1.5\,\text{Å}$, Twist angle = $\Delta\phi = \frac{5\pi}{9}$. The on-site energy for the helical chain (ε_0) and lead (ε_l) are chosen to be zero. The local magmetic moments are assumed to be equal on every sites and the value is $h = 1.0$ eV. Hopping integral between sites 1 and 2 are t_{11} = 1.0 eV,and the nearest neighbor hopping between the sites of the leads = t_l = 2.0 eV. Molecule to coupling is = $\tau_1 = \tau_2 = 0.75$ eV. All the results in this dissertation are worked out in the high frequency regime $\hbar\omega >> t_{11}$.

- ***Variation of total Charge Conductance ($G_c = G_\uparrow + G_\downarrow$) as a function of Fermi energy (E_F):***

Figure 3 shows the variation of electrical conductance (G) as a function of Fermi energy (E_F) for a 10-site LRH magnetic helix. We find several conductance peaks associated with the energy eigenvalues of the system. The peaks are broadened because here we have considered strong lead-conductor coupling limit. The key observation is that, the conductance peaks are non-uniformly distributed about $E_F = 0$. For $E_F \le 0$ the conductance peaks are densely packed, while the separation between the peaks increases for $E_F > 0$.

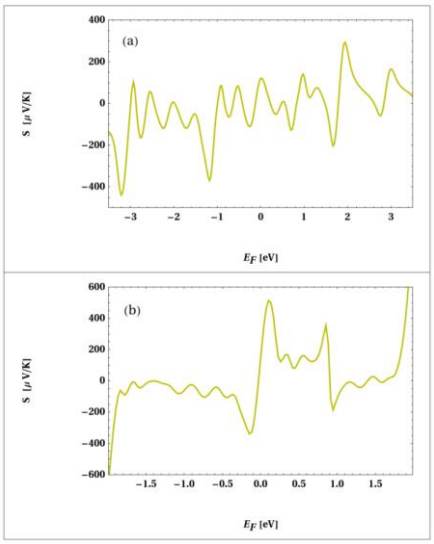

Figure 4: Seebeck coefficient (thermopower S) as a function of Fermi Energy (E_F) for a long-range hopping (LRH) magnetic helix in (a) absence and (b) presence of light. Here, we set N = 10 and A_0 = 0.5.

This is due to breaking of particle-hole symmetry and is the generic feature of long-range hopping models. The other notable observation is that, at some typical Fermi energies the conductance is highly asymmetric which is one of the essential criteria to have favorable thermoelectric response that can be understood from the expression of Landauer integrals.

The situation becomes more interesting when we irradiate the magnetic helix by a circularly polarized light. The overall conductance window gets narrowed due to the renormalization of hopping integral parameters in presence of high frequency radiation.

Moreover the conductance function becomes more asymmetric compared to the irradiation free case. This is one of our requirements.

- ***Variation of total Thermopower ($S_c = S_\uparrow + S_\downarrow$) as a function of Fermi energy (E_F):***

The results of thermopower are presented in fig 3.2 for both irradiated and radiation free cases of a 10 site LRH magnetic helix. In absence of irradiation the overall thermopower is quite small (~ 200 μV/K), specially towards the band centre whereas the thermopower gets reasonably enhanced in presence of irradiation. More specifically it is observed across $E_F = 0$.

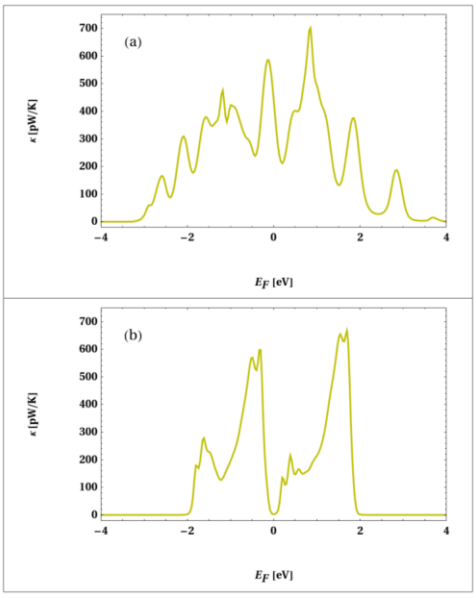

Figure 5: Thermal Conductance as a function of Fermi Energy (E_F) for a long-range hopping (LRH) magnetic helix in (a) absence and (b) presence of light. Here, we set N = 10 and A_0 = 0.5.

Finding higher thermopower towards the band centre is always favourable keeping in mind the experimental realization. Higher thermopower will yield large ZT as can be understood from the definition of FOM.

- ***Variation of total thermal conductance ($\kappa_{el} = \kappa_\uparrow + \kappa_\downarrow$) and charge figure of merit (ZT) as a function of Fermi energy (E_F):***

Figure 5 shows the dependence of thermal conductance (κ) on Fermi energy (E_F) for both irradiation free and irradiated cases of a 10 site LRH magnetic helix. Overall the spectra look quite similar like what are presented in fig 3.1, as expected. Comparing the spectra, fig 3.2 and fig 3.3, we find that at the typical Fermi energies where the thermopower is reasonably large, the thermal conductance (κ) is quite small for the irradiated magnetic helix. Because of this fact, we get significantly large (ZT), around the band centre as can clearly be observed from fig 6.

In absence of irradiation the overall ZT for the entire Fermi energy window is reasonably small. On the hand ZT reaches close to the desired value 4 when we irradiate the magnetic helix by a circularly polarized high frequency radiation. This is undoubtedly a very good observation as far as applications are concerned.

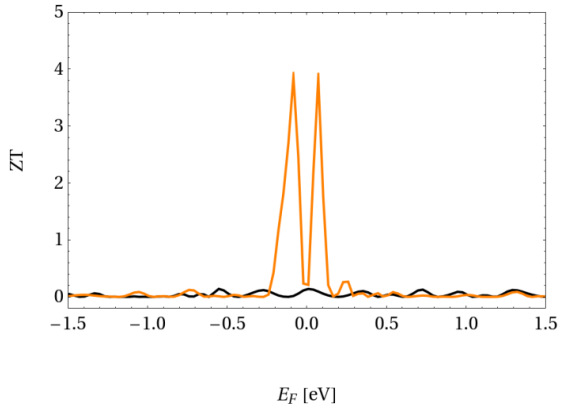

Figure 6: FOM as a function of Fermi Energy (E_F) for a long-range hopping (LRH) magnetic helix in absence (shown by black line) and (b) presence (shown by orange curve) of light. Here, we set N = 10 and A_0 = 0.5.

IV . Conclusion

To conclude, in the present work we have investigated thermoelectric phenomena at quantum level using a magnetic helix with long-range hopping interaction in presence of circularly polarized light irradiation. It includes the outline of thermoelectric phenomena describing the significance of considering low dimensional quantum systems circumventing the use of conventional bulk materials. It has already been established that bulk materials are not suitable enough for efficient energy conversion due to the constraint of Wiedemann-Franz law, where both the electrical and thermal conductances simultaneously either increase or decrease. On the other hand, these two quantities can be regulated independently at nano-scale level which leads to a possibility of suitable energy conversion. Moreover, a suitable tuning of FOM

provides an additional advantage in designing controlled thermoelectric engines. This article contains

a detailed mathematical description for the calculation of all the thermoelectric quantities. A thorough description of Bloch-Floquet formalism to incorporate the effect of irradiation on transmission related quantities is given, for the benefit of general readers. Simulating the quantum system within a tight-binding framework we compute all the thermoelectric quantities for a LRH magnetic helix using Landauer integrals. The spin resolved two terminal transmission probabilities are determined following the well known Green's function technique. In the numerical results, we have critically analysed all the essential results. Several noteworthy features are observed. We have found that, conductance peaks are non-uniformly spaced around zero Fermi energy. The peaks are highly asymmetric especially in the presence of light irradiation. The thermopower significantly increases towards the band centre and at the same time the thermal conductance gets suppressed enormously around $E_F = 0$ for the irradiated magnetic helix. As a result of this we have got a reasonable response in ZT which shows that it reaches very close to 4, which is the desired value for industrial purpose.

Our analysis might be helpful in studying thermoelectric behaviour in different kinds of short and long range helical geometries and similar kind of fascinating systems.

References

[1] Polcyn A, Khaleel M. (2009) Advanced Thermoelectric Materials for Efficient Waste Heat Recovery in Process Industries, Technical Report U.S. Department of Energy, Office of Scientific and Technical Information.

[2] Seebeck T. J. (1825), Magnetic polarization of metals and minerals by temperature differences, Treatises of the Royal Academy of Sciences in Berlin, (265-373).

[3] Chao K. A. and Larsson M. (2007), Physics of zero- and one-dimensional nanoscopic system, pp (156-168) of Solid State Sciences, Springer (2007).

[4] J. Peltier, Ann. Chim. (1834), Nouvelles Experiences sur la Caloriecete des Courans Electrique, L VI 371-387.

[5] H. J. Goldsmid (1964), Thermoelectric refrigeration, Plenum, New York.

[6] A. F. Ioffe (1957), Semiconductor thermoelements and thermoelectric cooling, Infosearch limited, London.

[7] Y. Dubi and M. Di Ventra (2011). Colloquium: Heat flow and thermoelectricity in atomic and molecular junctions, Rev. Mod. Phys. 83, 131-154.

[8] G. Chen (2005), Nanoscale energy transport and conversion, Oxford University Press, New York.

[9] A. Majumdar (2004).Thermoelectricity in Semiconductor Nanostructures, Science 303, 777-778.

[10] P. Rodgers (2008). Silicon goes thermoelectric, Nature Nanotechnology News and Views. 3, 76.

[11] L. E. Bell (2008). Cooling, heating, generating power, and recovering waste heat with thermoelectric systems, Science 321, 1457-1461.

[12] N. A. Zimbovskaya (2016). Seebeck effect in molecular junctions, J. Phys.: Condens. Matter 28, 183002 (26 pp).

[13] L. D. Hicks and M. S. Dresselhaus (1993). Effect of quantum-well structures on the thermoelectric figure of merit, Phys. Rev. B 47, 12 727-731.

[14] L. D. Hicks and M. S. Dresselhaus (1993). Thermoelectric figure of merit of a one-dimensional conductor, Phys. Rev. B 47, 16631-34.

[15] D. Segal and A. Nitzan (2005). Spin-Boson Thermal Rectifier, Phys. Rev. Lett. 94, 034301-5.

[16] N. Yang, G. Zhang, and B. Li (2009). Thermal rectification in asymmetric graphene ribbons, Appl. Phys. Lett. 95, 033107-10.

[17] L. Wang and B. Li (2008). Thermal Memory: A Storage of Phononic Information, Phys. Rev. Lett. 101, 267203-7.

[18] L. Wang and B. Li (2007). Thermal Logic Gates: Computation with Phonons, Phys. Rev. Lett. 99, 177208-12.

[19] B. Li, L. Wang, and G. Casati (2006).Negative differential thermal resistance and thermal transistor, Appl. Phys. Lett. 88, 143501-3.

[20] A. Shakouri (2006). Nanoscale Thermal Transport and Microrefrigerators on a Chip, Porc. IEEE 94, 1613-1638.

[21] A. I. Hochbaum, R. Chen, R. D. Delgado, W. Liang, E. C. Garnett, M.Najarian, A. Majumdar, and P. Yang (2008). Enhanced thermoelectric performance of rough silicon nanowires, Nature 451, 163-167.

[22] A. I. Hochbaum and P. Yang (2010). Semiconductor Nanowires for Energy Conversion, Chem. Rev. 110, 527-546.

[23] C. Yu, Y. S. Kim, D. Kim, and J, C. Grunlan (2008). Thermoelectric Behavior of Segregated-Network Polymer Nanocomposites, Nano Lett. 8, 12, 4428-4432 .

[24] E. Zerah-Harush and Y. Dubi (2015). Enhanced Thermoelectric Performance of Hybrid Nanoparticle–Single-Molecule Junctions, Phys. Rev. Appl. 3, 064017-8.

[25] N. Sergueev, S. Shin, M. Kaviany, and B. Dunietz (2011). Efficiency of thermoelectric energy conversion in biphenyl-dithiol junctions: Effect of electron-phonon interactions**,** Phys. Rev. B 83,195415 (1) -12.

[26] M. Galperin, A. Nitzan, and M. A. Ratner (2008). Inelastic effects in molecular junction transport: scattering and self-consistent calculations for the Seebeck coefficient, Mol. Phys. 106, 397-404.

[27] A. I. Boukai, Y. Bunimovich, J. T.-Kheli, J.-K. Yu, W. A. GoddardIII, and J. R. Heath (2008). Silicon nanowires as efficient thermoelectric materials, Nature 451, 168-171.

[28] J. P. Small, K. M. Perez, and P. Kim (2003). Modulation of Thermoelectric Power of Individual Carbon Nanotubes, Phys. Rev. Lett. 91, 256801-4.

[29] W. J. Kong, L. Lu, H. W. Zhu, B. Q. Wei, and D. H. Wu (2005). Thermoelectric power of a single-walled carbon nanotubes strand. J. Phys.: Condens. Matter 17, 1923-1928.

[30] P. Reddy, S.-Y. Jang, R. A. Segalman, and A. Majumdar (2007). Thermoelectricity in molecular junctions. Science 315, 1568-71.